ICE, CLOUD, AND LAND ELEVATION SATELLITE-2 (ICESat-2)
ATL12 Ocean Surface Height Release 001
Application Notes and Known Issues

James Morison
6/4/2019

Rev 1.0

Introduction

This document contains notes for the use of the ICESat-2 ATL12 Ocean Surface Height product. It includes issues that are known to the developers, which may be fixed in future releases of this product. Feedback from the community will be added to future revisions of this document.

Contents

Notes: The ATL12 Ocean Surface Height Product Philosophy and Brief Description

The Ice, Cloud, and Land Elevation Satellite-2 (ICESat-2) provides satellite ocean altimetry unlike any other. ICESat-2 has been developed primarily to measure the height of the Earth's ice and land at high spatial resolution. To achieve this resolution it carries the Advanced Topographic Laser Altimeter System (ATLAS), a photon-counting, multi-beam lidar pulsing at 10 kHz. At the speed of the spacecraft, each beam of ATLAS illuminates 15 m patch of the surface every 0.7 m of along-track distance. Given the low reflectance of the ocean surface, of all the photons detected by ATLAS, on the order of one photon per pulse returns from the ocean surface. ATLAS determines the apparent height of the reflecting surface for each one of these photons along with the apparent height of a lower density of noise photons. Averaged over along-track distance these heights form a histogram of heights reminiscent of the waveforms of other radar (e.g., CryoSat-2) and analog lidar (e.g., ICESat-1) satellite altimeters, and thus we are tempted to think in terms of "retracking" to decide what part of this "waveform" represents the average ocean surface over a "foot print" corresponding to the averaging distance.

We have adopted a different philosophy in processing the ICESat-2. We do not think in terms of "footprint" and "retracking" in the usual way, but treat every photon height documented in the ATL03 data product input to ATL12 as an individual point measurement of surface height averaging less than a meter apart, but with a x-y location uncertainty on the order of 10 m. Figure 1 shows ATL03 photon heights collected over 7-km of ocean surface. The dense cloud of heights representing surface-reflected photons clearly stands out from the lower density of noise photons above and below and reveals surface waves with about 2.5 m significant wave height (SWH) and an apparent 470-m wavelength. In processing, we first distinguish by a histogram trimming method, which of these heights over an adaptively chosen ocean segment length (typically 7-km) are from true surface reflected photons versus noise photons. The resultant "received height histogram" is deconvolved with an instrument impulse response (IIR) histogram representing the height uncertainty associated with the lidar transmit pulse width and other instrumental factors. This produces a surface height histogram that, with its first four moments, is the primary ATL12 products. In addition we analyze the spatial series of surface photons heights to characterize surface waves and calculate the correlation of photon return rate and surface height that constitutes the EM sea state bias (SSB) in the mean sea surface height (SSH).

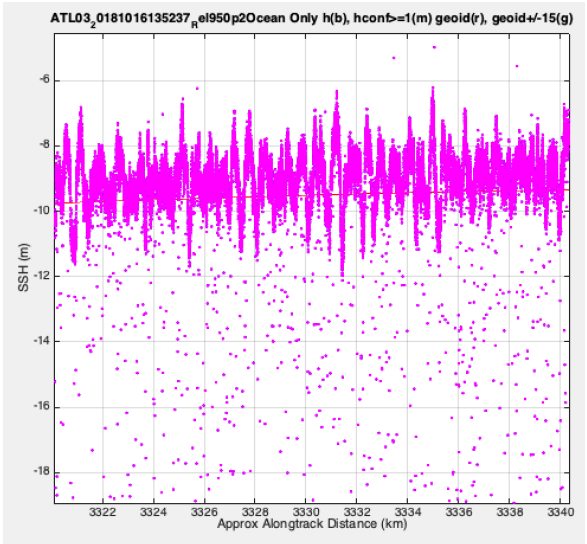

Figure 1. ATL03 photon heights (magenta) from Oct. 16, 2018 over the Pacific Ocean and the EGM2008 geoid (red line). Waves in the dense photon cloud are apparent as well as subsurface and atmospheric noise photons.

Thus, the ATL12 Ocean product includes histograms and statistics of sea surface height over variable length

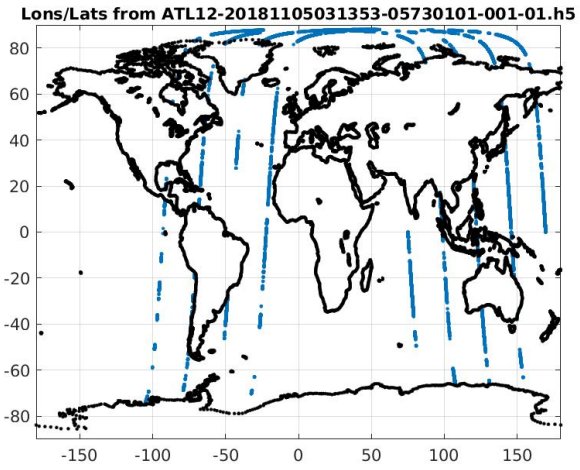

Figure 2. Example of one ATL12 file's worth of ocean segment latitudes and longitudes over four orbits comprising the file.

along-track ocean segments. ATL 12 photon heights are derived from the ATL03 ocean photon height data with signal confidence level 1 or higher and within 15 m of the EGM2008 geoid. Signal confidence 2, 3, and 4 correspond to low, medium, and high confidence the photon is surface reflected and confidence level 1 fills a ±15-m buffer about the high confidence level photon heights. This constraint, along with the geoid band criteria, have been found to edit out heights in erroneous downlink bands associated with high background noise rates.

From this population, we first accumulate photon heights likely to fall within the distribution of ocean surface heights until 8,000 candidate photons or 7 km of along-track distance is traversed. All the photons over the resulting ocean segment are then subjected to two iterations selecting photon heights in the histogram at levels above the background rate. After the first iteration, a linear trend and average height is removed from the heights prior to the second iteration. The trend and average height are retained for output as part of the ocean segment statistics. From there the height data follows two paths

The histogram path considers the histogram of the

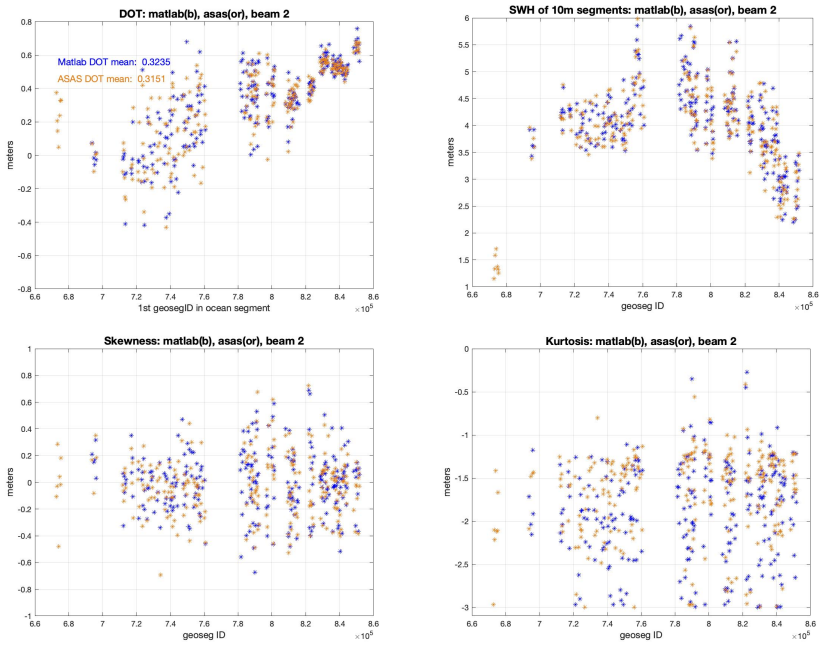

Figure 3 ATL12 ocean segment statistics. Upper left: mean SSH, upper right: significant wave height = 4 x standard deviation, lower left: skewness of sea surface height, lower right: kurtosis of sea surface height. Yellow DOTS are ATL12 ASAS 5.1 and blue dots are from our developmental Matlab code applied to ATL03, which generally does not segment the data exactly the same as ATL12. ASAS 5.1 and Matlab agreement is better where segments are more closely matched.

received ocean segment heights and deconvolves the histogram of the instrument impulse response to produce the surface height distribution. This is then fit with a 2 Gaussian mixture to produce the first four moments of the surface height distribution. The derived height surface histogram and the four moments comprise the main the ATL12 data products

The space series track maintains the surface heights as an along-track series and by correlating the photon return rate with surface height at 10-m along-track scale, estimates significant wave height and the EM sea state bias (SSB) ATL12 data products. In future releases, analyses on this track will include more wave properties and estimates of statistical degrees of freedom for the accumulation gridded statistics in the ATL17 gridded data product.

Each ATL12 data file covers the world ocean over four consecutive ICESat-2 orbits (Fig. 2). ATL12 file names such as ATL12_20181105031353_05730101_001_01.h5 include the date/time sequence (yyyymmddhhmmss=20181105031353) of the start of the first orbit, the reference ground track (_####=_0573), the cycle (##=01), the region (##=01), and the release (###=001).

The processed data are for areas designated as ocean according to the ICESat-2 ocean surface mask. The ocean mask overlaps with all the other surface types in buffer zones up to 20-km wide. Consequently, ATL12 data includes bands that are in fact not open ocean but which are close enough to sea level to fall within ±15 m of the geoid to be accepted by ATL12's processing. Examples are the marginal sea ice zones under the sea ice surface type and low-lying islands under the land surface type. Future revisions are to include a bathymetric test to insure the ATL12 processing covers only ocean waters.

Except in special cases or when overlapping one of the other surface types, over the ocean only the three strong beams with ground tracks separated by 3 km are downlinked by ATLAS. The ATL12 software processes each strong beam independently. An example of ocean statistics measure by the middle strong beam over one ATL03 granule in the North Pacific is shown in Figure 3 for all ocean segments in the granule.

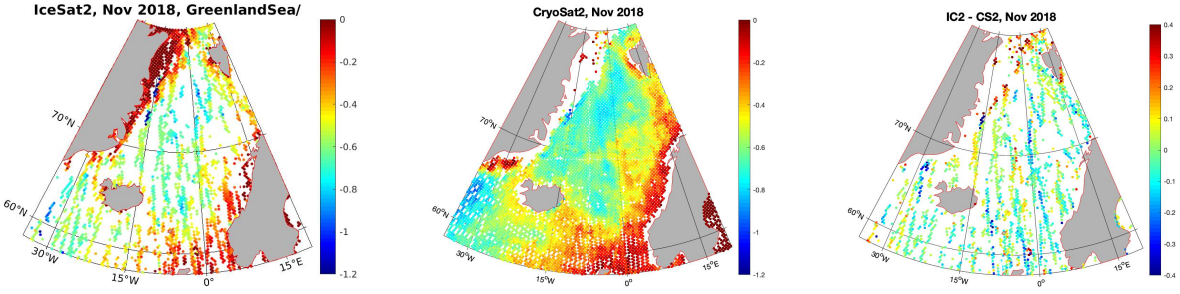

Figure 4. ICESat-2, CryoSat-2 dynamic ocean topography (DOT in meters) comparison for the Greenland Sea in November 2018. Left: ICESat-2 from ATL12 Rel001, bin-averaged in a 25-km grid. In this case ocean and sea ice mask data are included. Center: CryoSat-2 LRM and pLRM from RADS bin-averaged in a 25-km grid. These are open water products. Right: ICESat-2 DOT minus CryoSat-2 DOT bin-averaged in a 25-km grid. Differences are taken only for grid cells with both ICESat-2 and CryoSat-2 data.

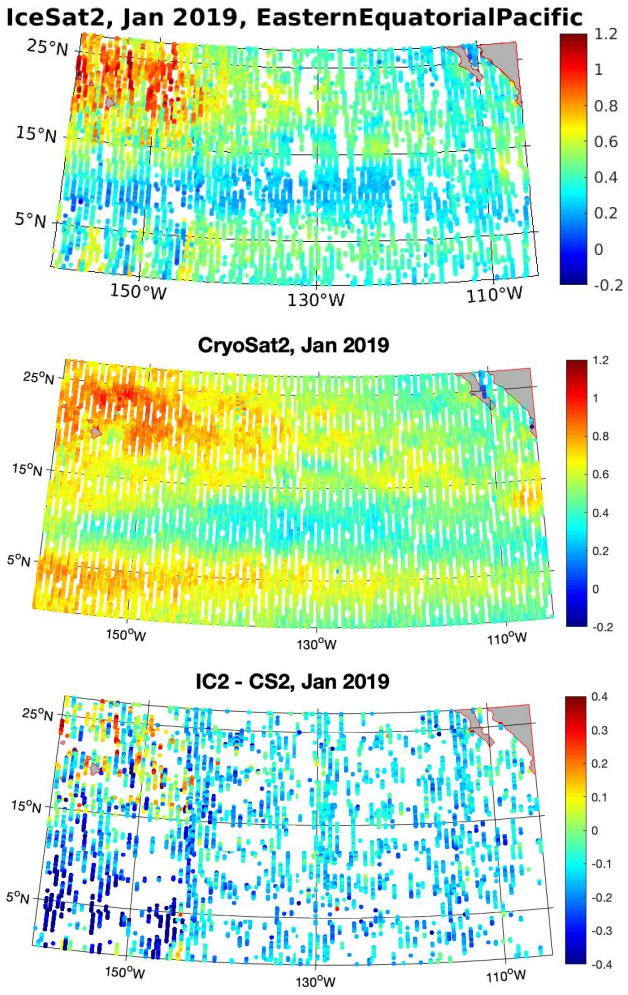

Figure 5. ICESat-2, CryoSat-2 dynamic ocean topography (DOT) comparison for the Eastern Equatorial Pacific in January 2019. Top: ICESat-2 DOT (m) from ATL12 Rel001, bin-averaged in a 25-km grid, Center: CryoSat-2 DOT (m) LRM and pLRM from RADS bin-averaged in a 25-km grid, Bottom: ICESat-2 DOT minus CryoSat-2 DOT (m) bin-averaged in a 25-km grid. Differences are taken only for grid cells with both ICESat-2 and CryoSat-2 data.

Our first efforts at calibration and validation of ICESat-2 SSH show good agreement with CryoSat-2, especially in the Sub-Arctic Seas. Figure 4 shows comparison of ICESat-2 and CryoSat-2 dynamic ocean topography, DOT=SSH-Geoid (EGM08) for the month of November 2018 bin-averaged in a 25-km grid. ICESat-2 did not get as many surface measurements as CryoSat-2, almost surely due cloud cover over the November Greenland Sea. However, the same DOT patterns such as DOT set up towards the coasts associated with the East Greenland, Norwegian, and West Spitzbergen currents are almost identically shown in both data sets. The difference between gridded ICESat-2 and CryoSat-2 DOT is on the right of Figure 4. Over all the grid cells with ICESat-2 and CryoSat-2, ICESat-2 DOT is 0.64 cm higher than CryoSat-2 DOT ± 16.6 cm standard deviation. This comparison is remarkable given the early release of ICESat-2.

Figure 5 is similar to Figure 4 except the comparison is done for the Eastern Equatorial Pacific (EEP) for January 2019. In spite of a lower density of ground tracks at low latitude, ICESAt-2 data coverage in the EEP is arguably better than in the Greenland Sea, likely because of clearer sky conditions. The ICESat-2 and CryoSat-2 DOT patterns in the EEP are very similar, showing among other things the trough along 5°N likely associated with North Equatorial Current and North Equatorial Counter Current. The similarity breaks down a little in the western part of the area with ICESat-2 DOT being a little higher than CryoSat-2 DOT in the northwest and lower than CryoSat-2 DOT in the southwest. On average ICESat-2 DOT is 13.1 cm lower than CryoSat-2 DOT ±12.2 cm standard deviation. This is not as good as the Greenland Sea comparison but comparable in magnitude to other ICESat-2 ground truth comparisons for this release.

Issues

The issues below are those that could affect use of ATL12 Rel. 001 presently or could affect changes in the way ATL12 data are used in the future.

Issue 1. Missing Ocean Segments

Due to issues solely with the ASAS 5.1 software, users may find occasional data gaps with missing ocean segments in ATL12 Rel. 001. The sources of these gaps are known and have been corrected in the newest generation of the code

Issue 2. Surface Finding, Subsurface Returns, and Histogram Trimming

Distinguishing surface reflected photon heights involves establishing a histogram of all heights in an ocean segment and then searching outward from the center of the histogram to find high and low limits where the histogram level falls below an estimate of the noise level. The photon heights between the high and low limits are considered surface photon heights. To determine the high and low limits, the current release (R001 - ASAS 5.1) compares a smoothed version of the histogram to the median value of the smoothed histogram. Because with the small binsize (1-cm) of the current processing, the median of the smoothed histogram usually reflects the noise tails, and the resulting trimming works reasonably well. However, it treats the subsurface and above surface tails of the histogram the same.

Because the blue-green laser of ATLAS penetrates water, true subsurface returns have always been a concern, and the higher subsurface density of photons apparent in Figure 1 may be due in part to subsurface scattering in the ocean. However, we see similarly enhanced subsurface densities over, clear deep ocean waters and even over land where penetration and backscatter shouldn't occur. Consequently present thinking expressed in the ATL03 known issues is that the subsurface noise level is due to forward scattering delays in the atmosphere of surface reflected photons.

Whatever their cause, some subsurface photon heights are being included in the surface height histogram, creating what we think may be an order 1-3 cm bias in average SSH. To reduce the sensitivity to subsurface returns, the present developmental code first makes a simple estimate of the high and low histogram limits and then uses these to determine separate above surface and subsurface noise levels. The ultimate high limit is then chosen where the smoothed histogram falls below a factor (e.g., 1.5) times the above surface noise and low limit is chosen where the smoothed histogram falls below the same factor times the subsurface noise. This method of reducing subsurface returns will be in future releases. We also plan to use a histogram for surface finding based on height departures from a smoothed high confidence photon surface to eliminate subsurface returns from under the crests of waves.

Issue 3. Uncertainty in Mean SSH

We have found the wave environment, rather than instrumental factors, is probably the biggest contributor to uncertainty in estimates of the mean SSH. This is illustrated by our analysis of multiple ocean segments, of which the data of Figure 1 is one 7-km ocean segment in the southern part of the central North Pacific. These segments show variability

in their mean sea surface heights of approximately ± 0.12, much greater than we'd expect from instrumental factors. The standard error, σ_L, in the estimates of the mean are given by

$$\sigma_L = \sigma_h \left(N_{df} \right)^{-1/2}$$

where σ_h is the standard deviation of the population and N_{df} is the number of degrees of freedom. If every one of the ~ 8,000 photon heights were independent, even with a SWH = 2.5 m (σ_h = .625 m), the uncertainty in estimates of the mean would be less than 1 cm. The problem is that owing presence of long large waves, successive photon heights are far from independent. The fact that the underlying wave signal is periodic makes the estimate of the effective degrees of freedom in terms of correlation length scale more problematic. As a worst case if we set N_{df} equal to the number of wave periods in the ocean segment, 15 in the case Figure 1, the uncertainty, σ_L, in the estimate of the mean equals 0.16 m, close to what we see over many similar ocean segments. This problem is not instrumental; it is just made apparent by the ability of ICESat-2 to resolve waves. To lower this uncertainty, we are exploring using harmonic analysis of surface height over each ocean segment and use of the zero wave-number amplitude to represent SSH (D. Percival, personal communication, 2019) as a way of removing large periodic variations in height as a cause of uncertainty. A further advantage of this approach will be that it will add a measure of wave spectral properties to ATL 12. In any event, we will have to derive measures of the effective number of degrees of freedom as an ATL12 output for each ocean segment in order to properly account for uncertainties in the ATL19 gridded SSH product.

Issue 4. Erroneous Downlink Bands

In order to conserve bandwidth over the ocean, the Flight Science Receiver Algorithms (FSRA) on board ICESat-2 select photons in a downlink band currently 30-m in vertical width (See ATL03 Users Guide). This band is centered over where FSRA detects the highest concentrations of photons. As long as the background photon count is low at night or in clear conditions this band will be centered on the ocean surface near the geoid. But in daylight with scattered clouds, the downlink band can shift to unrealistic heights or depths for 200-pulse major frames. To edit these erroneous downlink bands (EDB), ASAS 5.1 selects a band that includes photons with a signal confidence greater than or equal to 1. Signal confidence equal to 2, 3, 4 correspond to low, medium, and high confidence that the photon is a surface return. Signal confidence equal to 1 is applied to the remaining no confidence photons filling a band±15m around the high confidence photons. This confidence level filter, along and considering photons only within ±15 m of the geoid usually filters out the erroneous downlink bands, but there may be occasions where this doesn't work and some photons from EDB leak into consideration.

To address these issues the FSRA team has recently run an experimental FSRA on board ICESat-02 for about a day. Among other things, the experimental FSRA expanded the vertical width of the downlink band and now allows the downlink of photons in some sort of band when it finds no concentration of photon heights. We have to test how the ASAS ATL12 code responds to this FSRA change and adapt to it.

Issue 5. Sea Surface Heights Among Beams

Our cal/val comparisons with CryoSat-2 (Figs. 4 and 5) have been performed for the center strong beam only. We have not done a detailed study of leveling SSH across the three strong beams, but in two granules we used for comparisons between the ASAS 5.1 code and developmental Matlab code (e.g., Fig 3), we found beam 1 was 4 cm lower than the center beam and beam 3 was 4 cm higher than the center beam. We will be comparing results among the three strong beams and CryoSat-2 over wider areas and times in the near future.

Issue 6. Bathymetry Test and Surface Type

As mentioned in the notes, future revisions are to include a bathymetric test to insure the ATL processing covers only ocean waters. In the current ATL12 Rel. 001, the user may find data actually collected over low-lying land surfaces that are included in the ocean-land boundary buffer zone. The user can gain an appreciation of how much non-open ocean is included in an ocean segment by looking at the *gtxx/ssh_segments/stats/surf_type_prcnt* output variable that gives the percentage of the ocean segment covered by each surface type covered in an ocean segment. (Be advised that the surface type from 1 to 5 denote land, ocean, sea ice, land ice, and inland water as listed in ATL03, but the description in ATL12 RTel001 is misstated by reversing the order of land ice and sea ice). In the future, ASAS will include ocean depth from the GEBCO static gridded world ocean bathymetry and will process data as ocean data for depths greater than a threshold depth such as 10 m.

Issue 7. SSB Calculation

We estimate the Sea State Bias (SSB) due to variations in sampling over surface waves. The EM sea state bias occurs for example if more photons tend to be returned from wave troughs than from wave crests. This SSB is equivalent to the covariance of photon return rate and sea surface height divided by the average photon return rate. We estimate this with the return rates and heights averaged in 10-m along track bins. The SSB estimates have been smaller than we have expected ~-1.2 % of Significant Wave Height (SWH) for our developmental code and about half that for the ATL12 data. Typical radar altimeters show an SSB of about – 4% and we have found ICESat-2 to have no SSB below SWH= 2 m, but -18% f=of SWH above 2 m [*Morison et al.*, 2018]. Therefore, we will investigate the differences in the Matlab and ASAS code computations of SSB and also compare the rate based SSB to comparison of photon average heights to averages of 10-m bin averages that should be less prone to SSB.

Issue 8. High freeboard samples due to sea state

Related to the SSB Calculation issue, ATL07 results near the ice edge sometimes show reduced SSH near the ice edge. It has been hypothesize that this is due to strong photon returns from quasi-specular returns from ice crystals collected in the troughs of waves. We see some evidence of these depressions in the ATL12 data along the East Greenland ice edge and will test this hypothesis with our SSB calculation.

Issue 9. Lower transmitted energy in Beam 3 (Strong Beam)

According to the ATL07/10 results, the transmit energy of Beam 3 (Strong beam 2R or 2L, depending on orientation of the ICESat-2 observatory) is approximately 80% that of Beam 1 and Beam 5. Thus, the segment lengths and photon return rate may be different from the other two strong beams.

Issue 10. Cloud Flag Usage

The computation of the *layer_flag*, which combines the information in *cloud_flag_atm*, *cloud_flag_asr* and *bsnow_con* into a consolidated flag for indication of cloud coverage, was implemented incorrectly in the current release (Rel. 001 - ASAS 5.1). DO NOT USE.
In connection with addressing Issues 1, 3, and 5 we will investigate using the ATL09 cloud coverage data to filter the altimetry data in future versions of ATL12.

Issue 11. Output of background Photon Rate

Also in connection with addressing Issues 1, 3, and 5, we will begin out putting photon background rate. The Ocean ATBD table 5.2 for the ATL12 output parameters has clarified the definition of background rate (*backgr_seg*) and specifies it as an output parameter to the *gtx/ssh_segments/stats* group.

Issue 12. Bin Boundary Definitions

Currently, the ATL12 bins are centered on even centimeters, e.g. for ±15 m, centers at 15.00 m, 14.99 m, … etc. However, the array of bin edges is only as long as the array of bin centers so the last bin ends up being half as wide as it should be. The length of the array of bin edges will be expanded by one.

Reference:
Morison J., R. Kwok, S. Dickinson, D. Morison, C. Peralta-Ferriz, and R. Andersen (2018), Sea State Bias of ICESat in the Subarctic Seas, *IEEE Geoscience and Remote Sensing Letters*, 15 (8), 1144 - 1148, DOI: 10.1109/LGRS.2018.2834362